Control of a Helicopter Laboratory Process using Fuzzy Techniques

Oscar Mauricio Agudelo*, Jairo José Espinosa†, and Joos Vandewalle‡

Abstract

This document presents the results of applying linear and fuzzy control techniques on a 2 degrees of freedom helicopter known as *COPTER II*. Initially a Linear Quadratic Gaussian (LQG) controller was designed from the linear model of the plant. This model was estimated by using multivariable identification techniques. Afterwards a fuzzy controller was derived. This controller takes into account the nonlinear characteristics of the setup. The fuzzy control system was developed from the Takagi-Sugeno (TS) fuzzy model of the helicopter by using the concept of Parallel Distributed Compensation (PDC). This TS fuzzy model was constructed by integrating a set of linear models of the plant around different operating points. Likewise in the LQG case, the linear models were found by means of multivariable identification techniques.

Keywords: Fuzzy Control, Identification, Nonlinear Systems, Linear Quadratic Gaussian Control, Proportional control.

1 Introduction

Nowadays optimal control and fuzzy control techniques have evolved into powerful control methodologies, facing and solving challenging industrial control problems. In this paper we present an application of these powerful control techniques on a process that is characterized by fast dynamics and nonlinear behavior [1]. Moreover, this process is extremely difficult to control under manual operation, and it possess a considerable cross-coupling. This process is a challenging educational experiment, fairly adequate for evaluating and comparing different control schemes. The process is a 2 degrees of freedom helicopter known as *COPTER II* and it is depicted in Fig. 1. This setup was built at the Universidad Autónoma de Occidente [8] based on well-known commercial equipment offered by Quanser (2 DOF Helicopter), Humusoft (CE 150 Helicopter Model) and FeedBack Instruments (Twin Rotor MIMO System 33-007).

There have been several studies about the control of this kind of systems. In [6] the *CE 150 Helicopter Model* is controlled by means of a Model Predictive Controller (MPC). The MPC uses a linear model which is obtained by linearizing the nonlinear model of the helicopter around an operating point. The nonlinear model of the system is derived from first principles and the unknown parameters are identified. In [18] a practical design methodology to the stabilization of a 3 degrees of freedom (3-DOF) RC helicopter is presented. Using a Linear Matrix Inequality (LMI) approach, a Takagi-Sugeno (TS) fuzzy controller is designed via Parallel distributed Compensation (PDC) from the TS fuzzy model of the system. This fuzzy model is derived from the nonlinear model of the helicopter. In [3] and [4], black box identification techniques are used to find the mathematical model of a one degree of freedom *Twin Rotor MIMO System* (TRMS) which is operating in hover mode. In [4] the extracted model is employed in the design of a Linear Quadratic Gaussian (LQG) compensator. This LQG controller is combined with a feed-forward action in order to satisfy the performance objectives. Recently in [12] the development an adaptive dynamic non-linear model inversion control law for a *Twin Rotor MIMO System* (TRMS) utilizing artificial neural networks and genetic algorithms is studied. In this work a highly nonlinear one degree of freedom mathematical model of the TRMS is considered and a nonlinear inverse model is developed for the pitch channel. A genetic algorithm-tuned proportional-derivative (PD) controller is used to enhance the tracking characteristics of the system and an adaptive neural network element is integrated, thereafter, with the feedback control system to compensate for model inversion errors. Other recent applications of fuzzy modeling and control can be found in [5][9][19][20][21][23].

In this paper we present the design and implementation issues of an LQG regulator and a TS fuzzy controller for the helicopter laboratory process shown in Fig. 1. The control objective of both control systems is to track the setpoint changes of the 2 degrees of freedom of the helicopter, namely, the elevation and azimuth angles. Notice that we control the complete system, unlike other reported studies where only one degree of freedom (typically the elevation or pitch angle) is controlled [3][4][12].

*Department of Electrical Engineering (ESAT), Research Group SCD-SISTA, Katholieke Universiteit Leuven, Kasteelpark Arenberg 10, B-3001 Heverlee (Leuven), Belgium, and Department of Automation and Electronics, Universidad Autónoma de Occidente, Calle 25 No 115-85, Cali, Colombia. mauricio.agudelo@esat.kuleuven.be

†Facultad de Minas, Universidad Nacional de Colombia, Carrera 80 No. 65-223, Medellin, Colombia. jairo.espinosa@ieee.org

‡Department of Electrical Engineering (ESAT), Research Group SCD, Katholieke Universiteit Leuven, Kasteelpark Arenberg 10, B-3001 Heverlee (Leuven), Belgium. joos.vandewalle@esat.kuleuven.be

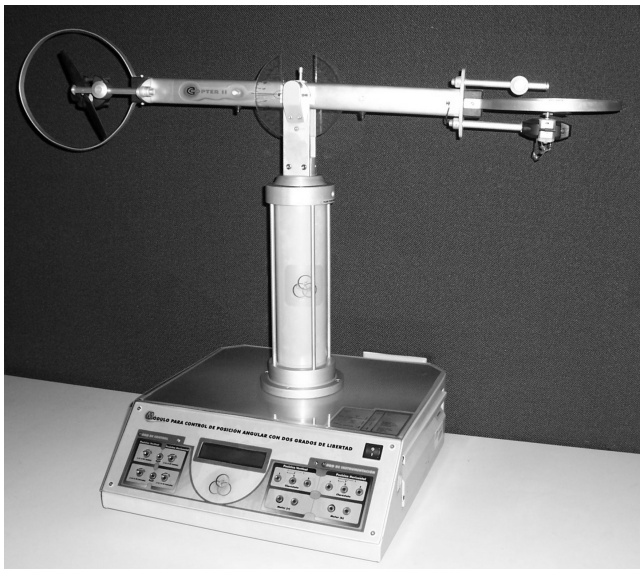

Fig. 1. Photograph of the Helicopter Laboratory Process.

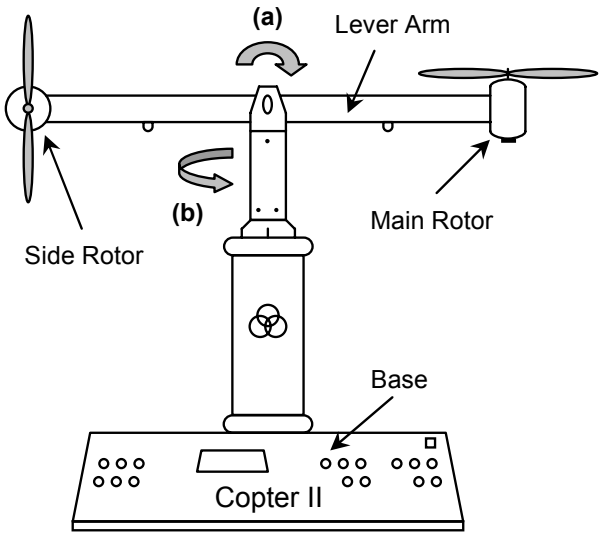

Fig. 2. Degrees of freedom of the Helicopter. a) Rotation of the lever arm (pitch or elevation angle). b) Rotation of the vertical axle (yaw or horizontal angle).

We have followed a very practical approach in the design of the fuzzy controller. As it is well known, the first step in the design of a TS fuzzy controller is the derivation of the TS fuzzy model of the process, which is nothing else than a nonlinear approximation of the rigorous nonlinear model of the plant. Typically this TS fuzzy model is constructed from several linear models which have been derived by linearizing the rigorous nonlinear model around different operating points. Although a rigorous nonlinear model of the *COPTER II* can be derived from first principles, many of the model parameters can not be measured directly, and they would have to be estimated by performing identification experiments similar to the ones presented in [6]. Alternatively, we can find directly the linear models on which the TS fuzzy model is based by means of system identification techniques. Therefore unlike [18] where the TS fuzzy model is built from the nonlinear model of the system, in our case the linear models on which the fuzzy model is based are obtained by means of the subspace identification algorithm N4SID [15], which has been properly configured to this end. Like in [3] and [4], the modeling is done assuming no prior knowledge of the model structure and its parameters. Once the TS fuzzy model is constructed, the fuzzy controller is designed via PDC as it is done in [18][22]. The procedure shown in this paper is a good alternative for designing TS fuzzy controllers when the nonlinear model of the process is not available.

Along this study, the LQG controller and the TS fuzzy controller incorporate integral actions in order to reduce the steady state errors to zero. From the practical point of view, it is important to implement an anti-windup mechanism in order to avoid that the integral terms wind up when the actuators are saturated, e.g. when the lever arm of the helicopter is held externally. In the literature there are not many references about the implementation of anti-windup systems for TS fuzzy controllers with integral action. Hence, in this manuscript we propose a systematic way of implementing the anti-windup mechanism for an LQG controller and a TS fuzzy controller.

The paper presents a description of the process in Section 2. Section 3 shows the design of the linear control system, including the identification of the plant, the tuning of the LQG controller and the design of the anti-windup system. In addition, the experimental results obtained with this control scheme are presented at the end of this section. Section 4 explains the identification of the fuzzy model and the design of the fuzzy controller using PDC as well as the stability test applied to the controller. Additionally, the main issues involved in the practical implementation of the fuzzy controller are explained and the experimental results are presented. Finally, Section 5 draws the main conclusions.

2 Plant Description

The process is shown in Fig. 1 and Fig. 2. In some aspects, the behavior of the *COPTER II* resembles the behavior of a real helicopter. From the control point of view it exemplifies a high-order nonlinear system with significant cross-coupling. The helicopter has a vertical axle, on which a lever arm is connected by a joint (the arm is pivoted). The lever arm represents the fuselage of the aircraft. The system has two degrees of freedom: the rotation of the lever arm (pitch or elevation angle) with respect to the vertical axle and the rotation of the vertical axle (yaw or azimuth angle) with respect to the fixed ground (see Fig. 2).

Two rotors are mounted on the lever arm, which are driven by DC Motors. Changes in the voltage applied to the motors will vary their rotation speed and therefore the aerodynamic forces generated by the rotors.

These resulting forces will change the elevation and azimuth angles of the helicopter. Hence, the helicopter is a multivariable system with two inputs (the voltages applied to the rotors) and two outputs (elevation and azimuth angles).

The main rotor has a major influence on the elevation angle, whereas the side rotor has its main influence on the azimuth angle. When a constant voltage is applied to the main rotor, the lever arm rotates until it reaches a steady final angle. However, when a constant voltage is applied to the side rotor, the vertical axle rotates with constant velocity until it reaches the physical limits of the system. Mathematically speaking, the last behavior indicates that the system has an "integrator" between the inputs (rotors) and the azimuth angle.

The system has two adjustable counterweights (see Fig. 1 and Fig. 8) affecting the process dynamics. However, the position of the counterweights is not measured and therefore we can not use it as part of the control strategies. In normal operating conditions the position of the counterweighs is established in such a way that the lever arm remains horizontal (see Fig. 8a), when no voltage is applied to the rotors. The elevation angle of the helicopter can be controlled in the range of -50 to 50 degrees and the azimuth angle can be controlled from -130 to 130 degrees. The signal conditioning circuits of the position sensors and the power drivers of the D.C motors are located inside the base of the *COPTER II*. The signal conditioning circuits of the sensors give variable voltages between -5 v and 5 v (linear relationship) and the power drivers of both motors have an input range from -5 v to 5 v. These features facilitate the connection of the helicopter to a generic data acquisition system.

3 Linear Control System

As it was mentioned before, initially we designed a Linear Quadratic Gaussian (LQG) controller from the linear model of plant around 0 degrees of elevation and azimuth angles. We derived such a linear model by means of multivariable system identification techniques. In the following subsections the identification of the helicopter and the design and implementation issues of the linear control system will be explained in detail.

3.1 Multivariable Identification of the process

In the identification experiment, Pseudo Random Binary Sequences (PRBS) were applied to the rotors of the helicopter and the helicopter response was registered. The sampling time (T_s) was fixed to 50 ms; this value is approximately 1/20 of the fastest time constant of the process.

The signals acquired from the helicopter were preprocessed in order to remove the DC level of the signals and the integral effect between the inputs and the azimuth angle. The helicopter model was derived in three steps [1][2]. In the first step, the model between the rotors and the elevation angle was obtained. This model is given by

$$\tilde{\mathbf{x}}(k+1) = \tilde{\mathbf{A}}\tilde{\mathbf{x}}(k) + \tilde{\mathbf{B}}\mathbf{u}(k) \qquad (1)$$
$$y_1(k) = \begin{bmatrix} 1 & 0 & 0 \end{bmatrix} \tilde{\mathbf{x}}(k)$$

with

$$\tilde{\mathbf{A}} = \begin{bmatrix} 0 & 1 & 0 \\ 0 & 0 & 1 \\ 0.808 & -2.61 & 2.802 \end{bmatrix}$$
$$\tilde{\mathbf{B}} = \begin{bmatrix} 2.007 \cdot 10^{-4} & -2.511 \cdot 10^{-4} \\ 3.86 \cdot 10^{-4} & -6.396 \cdot 10^{-4} \\ 6.548 \cdot 10^{-4} & -9.555 \cdot 10^{-4} \end{bmatrix}$$

where $\tilde{\mathbf{x}}(k) \in \Re^3$ is the state vector, $\tilde{\mathbf{A}} \in \Re^{3\times 3}$ and $\tilde{\mathbf{B}} \in \Re^{3\times 2}$ are the matrices describing the system dynamics, $y_1(k) \in \Re$ is the elevation angle and $\mathbf{u}(k) \in \Re^2$ is the input vector ($u_1(k)$ and $u_2(k)$ are the voltages applied to the main and side rotors respectively).

In the second step, the model between the rotors and the azimuth angle was found. Since the azimuth angle signal was differentiated in the preprocessing state (to get rid of the integral effect), we first estimated the model between the rotors and the azimuth angular velocity. We found the following model:

$$\breve{\mathbf{x}}(k+1) = \breve{\mathbf{A}}\breve{\mathbf{x}}(k) + \breve{\mathbf{B}}u(k) \qquad (2)$$
$$\dot{y}_2(k) = \begin{bmatrix} 1 & 0 & 0 \end{bmatrix} \breve{\mathbf{x}}(k)$$

with

$$\breve{\mathbf{A}} = \begin{bmatrix} 0 & 1 & 0 \\ 0 & 0 & 1 \\ 0.759 & -2.474 & 2.714 \end{bmatrix}$$
$$\breve{\mathbf{B}} = \begin{bmatrix} 0 & 1.947 \cdot 10^{-3} \\ 0 & 1.419 \cdot 10^{-3} \\ 0 & 1.388 \cdot 10^{-3} \end{bmatrix}$$

where $\breve{\mathbf{x}}(k) \in \Re^3$ is the state vector, $\breve{\mathbf{A}} \in \Re^{3\times 3}$ and $\breve{\mathbf{B}} \in \Re^{3\times 2}$ are the matrices describing the system dynamics, $\dot{y}_2(k) \in \Re$ is the azimuth angular velocity and $\mathbf{u}(k) \in \Re^2$ is the input vector. In order to obtain the azimuth angle an integrator ($T_s z/(z-1)$) was added to (2) as follows:

$$\begin{bmatrix} \breve{\mathbf{x}}(k+1) \\ x_s(k+1) \end{bmatrix} = \begin{bmatrix} \breve{\mathbf{A}} & \mathbf{0} \\ \mathbf{d}_1 & 1 \end{bmatrix} \begin{bmatrix} \breve{\mathbf{x}}(k) \\ x_s(k) \end{bmatrix} + \begin{bmatrix} \breve{\mathbf{B}} \\ \mathbf{d}_2 \end{bmatrix} \mathbf{u}(k) \qquad (3)$$
$$y_2(k) = \begin{bmatrix} 0 & 0 & 0 & 1 \end{bmatrix} \begin{bmatrix} \breve{\mathbf{x}}(k) \\ x_s(k) \end{bmatrix}$$

with

$$\mathbf{d}_1 = \begin{bmatrix} 0 & T_s & 0 \end{bmatrix} = \begin{bmatrix} 0 & 0.05 & 0 \end{bmatrix}$$
$$\mathbf{d}_2 = T_s \cdot \breve{\mathbf{B}}(1,:) = \begin{bmatrix} 0 & 9.735 \cdot 10^{-5} \end{bmatrix}$$

where $x_s \in \Re$ is the extra state introduced by the integrator, $\breve{\mathbf{B}}(1,:)$ denotes the first row of the matrix $\breve{\mathbf{B}}$, and $y_2(k) \in \Re$ is the azimuth angle.

Finally in the third step, the partial models (1) and (3) were put together in order to obtain the complete model (7th order) of the system,

$$\mathbf{x}(k+1) = \mathbf{A}\mathbf{x}(k) + \mathbf{B}\mathbf{u}(k) \tag{4}$$

$$\mathbf{y}(k) = \begin{bmatrix} 1 & 0 & 0 & 0 & 0 & 0 & 0 \\ 0 & 0 & 0 & 0 & 0 & 0 & 1 \end{bmatrix} \mathbf{x}(k)$$

with

$$\mathbf{A} = \begin{bmatrix} 0 & 1 & 0 & 0 & 0 & 0 & 0 \\ 0 & 0 & 1 & 0 & 0 & 0 & 0 \\ 0.808 & -2.61 & 2.802 & 0 & 0 & 0 & 0 \\ 0 & 0 & 0 & 0 & 1 & 0 & 0 \\ 0 & 0 & 0 & 0 & 0 & 1 & 0 \\ 0 & 0 & 0 & 0.759 & -2.474 & 2.714 & 0 \\ 0 & 0 & 0 & 0 & 0.05 & 0 & 1 \end{bmatrix}$$

$$\mathbf{B} = \begin{bmatrix} 2.007 \cdot 10^{-4} & -2.511 \cdot 10^{-4} \\ 3.86 \cdot 10^{-4} & -6.396 \cdot 10^{-4} \\ 6.548 \cdot 10^{-4} & -9.555 \cdot 10^{-4} \\ 0 & 1.947 \cdot 10^{-3} \\ 0 & 1.419 \cdot 10^{-3} \\ 0 & 1.388 \cdot 10^{-3} \\ 0 & 9.735 \cdot 10^{-5} \end{bmatrix}$$

where $\mathbf{x}(k) \in \Re^7$ is the state vector, $\mathbf{A} \in \Re^{7\times 7}$ and $\mathbf{B} \in \Re^{7\times 2}$ are the matrices describing the local dynamics, $\mathbf{y}(k) \in \Re^2$ is the output vector ($y_1(k)$ is the elevation angle and $y_2(k)$ is the azimuth angle) and $\mathbf{u}(k) \in \Re^2$ is the input vector ($u_1(k)$ and $u_2(k)$ are the voltages applied to the main and side rotors respectively).

For the partial models (1) and (2), a step response was used to determine the delays between the inputs and the output angle. Similarly, we estimated the order of (1) and (2) by calculating the singular values of their respective Hankel matrices. We used the subspaces algorithm N4SID [15] for performing the identification of (1) and (2). In both cases the algorithm was configured to generate the state space models in an observer canonical form. As consequence of this, the states $x_1(k)$ and $x_4(k)$ correspond to the elevation angle and the azimuth angular velocity respectively. Furthermore the state $x_7(k)$ represents the azimuth angle. The remaining states do not have a physical meaning, but they are required to properly describe the helicopter dynamics. The physical interpretation of some states facilitates the design of the LQG controller using the standard formulation.

Each partial model was validated according to the following criteria: the simulation and prediction errors (one sample ahead), the cancellations of poles and zeros and the residual analysis.

3.2 Design of the LQG control system

Linear Quadratic Gaussian control is a modern state space technique for designing optimal dynamic regulators. It enables us to tradeoff regulation performance and control effort, and to take into account process and measurement noise. An LQG regulator consists of a Linear Quadratic Regulator (LQR) and a Kalman Filter (optimal state estimator) [10]. The first step in the design of a LQG control system is to look for a state feedback law that minimizes the cost function

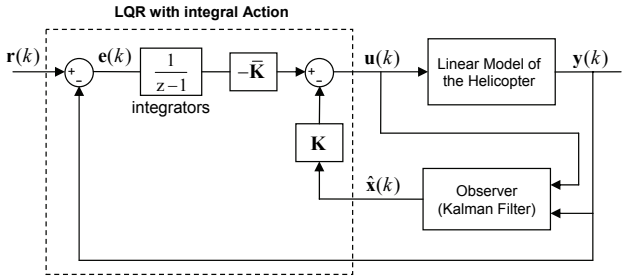

Fig. 3. LQG control system.

of regulation performance, which is calculated using a quadratic performance criterion with a set of user-specified weighting matrices which define the tradeoff between regulation performance and control effort. The next step is to derive a state space estimator using the Kalman filter theory. The optimal estimations of this Kalman filter would be used by the optimal state feedback law.

The block diagram of the LQG control system can be observed in Fig. 3. Since the controlled system must track the setpoint changes of the elevation and azimuth angles, it was necessary to construct the augmented model of (4) by introducing 2 integral terms as follows:

$$\begin{bmatrix} \mathbf{x}(k+1) \\ \mathbf{x}_\mathrm{e}(k+1) \end{bmatrix} = \begin{bmatrix} \mathbf{A} & \mathbf{0} \\ -\mathbf{C} & \mathbf{I} \end{bmatrix} \begin{bmatrix} \mathbf{x}(k) \\ \mathbf{x}_\mathrm{e}(k) \end{bmatrix} + \tag{5}$$

$$+ \begin{bmatrix} \mathbf{B} \\ \mathbf{0} \end{bmatrix} \mathbf{u}(k) + \begin{bmatrix} \mathbf{0} \\ \mathbf{I} \end{bmatrix} \mathbf{r}(k)$$

where $\mathbf{x}_\mathrm{e} \in \Re^2$ represents the extra states introduced to the system by 2 integral terms (integrator form: $1/(z-1)$) and $\mathbf{r}(k) \in \Re^2$ is the reference vector. The function of the integral terms is to reduce to zero the steady state errors of the elevation and azimuth angles. The control law (LQR with integral action) is given by the following equation,

$$\mathbf{u}(k) = -\mathbf{K}\mathbf{x}(k) - \bar{\mathbf{K}}\mathbf{x}_\mathrm{e}(k) \tag{6}$$

where

$$\mathbf{K}^T = \begin{bmatrix} 319.5495 & 4.7252 \\ -721.2870 & -9.4351 \\ 406.4029 & 4.3596 \\ 13.0902 & 107.4951 \\ -29.7839 & -246.0480 \\ 17.5491 & 146.1810 \\ 0.63 & 7.0729 \end{bmatrix} \text{ and}$$

$$\bar{\mathbf{K}} = \begin{bmatrix} -0.0768 & -0.0063 \\ 0.0066 & -0.0966 \end{bmatrix}.$$

The gains $\mathbf{K}$ and $\bar{\mathbf{K}}$ were calculated such that the control law given by (6) minimizes the cost function

$$J = \frac{1}{2} \sum_{k=0}^{\infty} \left(\bar{\mathbf{x}}^T(k) \mathbf{S} \bar{\mathbf{x}}(k) + \mathbf{u}^T(k) \mathbf{R} \mathbf{u}(k) \right)$$

$$\text{with} \quad \bar{\mathbf{x}}(k) = \begin{bmatrix} \mathbf{x}(k) & \mathbf{x}_\mathrm{e}(k) \end{bmatrix}^T$$

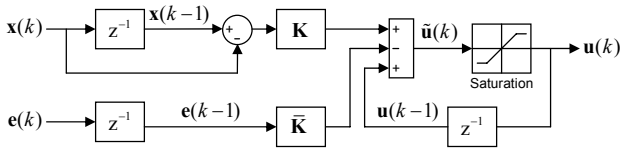

Fig. 4. Block scheme of the LQR Controller with integral action and anti-windup system.

subject to the state dynamics given by (5), with the following weighting matrices:

$$\mathbf{S} = \text{diag}\left(\begin{bmatrix} 5500 & 1 & 1 & 1 & 1 & 1 & 3500 & 2.5 & 3 \end{bmatrix}\right)$$
$$\mathbf{R} = \text{diag}\left(\begin{bmatrix} 400 & 300 \end{bmatrix}\right).$$

The matrix $\mathbf{S}$ penalizes the deviations of the process states whereas the matrix $\mathbf{R}$ penalizes the process inputs. These matrices have been found after a trial and error process, where we were looking for a closed-loop behavior without overshoot. Additionally along this procedure, we kept in mind that the states 1 and 7 are related to the elevation and azimuth angles and the states 8 and 9 are associated to the tracking errors.

The observer gain $\mathbf{L}$ was calculated in an optimal way (Kalman Filter) such that the covariance of the estimation error $(\mathbf{x}(k) - \hat{\mathbf{x}}(k))$ given by

$$J = \frac{1}{2}\varepsilon\left\{\sum_{k=0}^{\infty}\left(\mathbf{x}(k) - \hat{\mathbf{x}}(k)\right)^T\left(\mathbf{x}(k) - \hat{\mathbf{x}}(k)\right)\right\}$$

is minimized; where $\varepsilon\{\cdot\}$ represents the expected value. In the calculation of the observer gain, the following design matrices were used:

$$\mathbf{R}_{\text{v}} = \varepsilon\left\{\mathbf{v}(k)\mathbf{v}^T(k)\right\} = \begin{bmatrix} 3.4\cdot 10^{-6} & 0 \\ 0 & 1.3\cdot 10^{-6} \end{bmatrix}$$
$$\mathbf{R}_{\text{w}} = \varepsilon\left\{\mathbf{w}(k)\mathbf{w}^T(k)\right\} = \begin{bmatrix} 1 & 0 \\ 0 & 1 \end{bmatrix}.$$

Here, $\mathbf{R}_{\text{v}}$ is the covariance matrix of the measurement noise $(\mathbf{v}(k))$ and $\mathbf{R}_{\text{w}}$ is the covariance matrix of the process noise $(\mathbf{w}(k))$. The diagonal of $\mathbf{R}_{\text{v}}$ contains the measured noise variance of each output signal which were assumed to be uncorrelated. The noise variance of each output was estimated from the data collected when no voltage was applied to the rotors. Physically, $\mathbf{R}_{\text{w}}$ tries to explain unknown disturbances, whether they are steps, white noise, or imperfections in the model of the plant. This parameter can be used to trade speed and robustness. In this case, $\mathbf{R}_{\text{w}}$ was chosen to be equal to the identity matrix. The simulations and the experimental results confirmed that it was an appropriated choice for calculating the observer gain.

3.2.1 Anti-windup System

As it was mentioned in section 2, the helicopter inputs are limited between -5 to 5 volts. If the controller saturates the actuators, we have to stop the integration

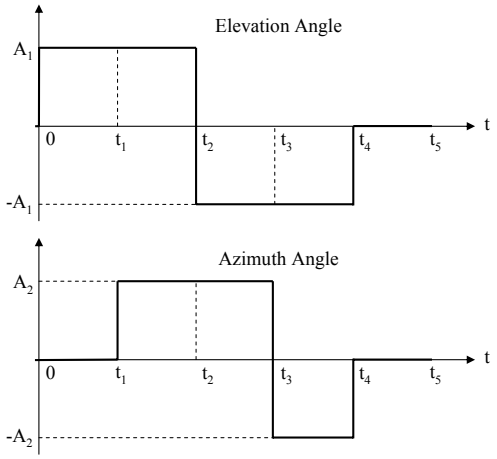

Fig. 5. Setpoint sequences for testing the controllers. $t_1 = 20$ sec, $t_2 = 40$ sec, $t_3 = 60$ sec, $t_4 = 80$ sec and $t_5 = 100$ sec.

mechanism in order to avoid that the integrators accumulate "extra control action" (wind up). Otherwise this "extra control action" would have to be removed later and the controlled system would exhibit an unnecessary overshoot and oscillations. In order to avoid this situation, an anti-windup system was designed for the controller.

The first step in the implementation of the anti-windup mechanism for the LQR controller with integral action is to transform it into a recursive form [1]. Firstly, the differences equation of the integral terms $(\mathbf{x}_{\text{e}}(k) = \mathbf{x}_{\text{e}}(k-1) + \mathbf{e}(k-1)$ from $1/(z-1))$ is replaced in (6) as follows,

$$\mathbf{u}(k) = -\mathbf{K}\mathbf{x}(k) - \bar{\mathbf{K}}\mathbf{x}_{\text{e}}(k-1) - \bar{\mathbf{K}}\mathbf{e}(k-1). \quad (7)$$

Given that equation (6) can be written in the following way

$$\mathbf{u}(k-1) = -\mathbf{K}\mathbf{x}(k-1) - \bar{\mathbf{K}}\mathbf{x}_{\text{e}}(k-1)$$
$$\mathbf{u}(k-1) + \mathbf{K}\mathbf{x}(k-1) = -\bar{\mathbf{K}}\mathbf{x}_{\text{e}}(k-1), \quad (8)$$

we can replace (8) in (7) in order to obtain the recursive version of the state feedback controller with integral action,

$$\mathbf{u}(k) = \mathbf{u}(k-1) + \mathbf{K}\left(\mathbf{x}(k-1) - \mathbf{x}(k)\right) - \bar{\mathbf{K}}\mathbf{e}(k-1). \quad (9)$$

The second and final step in the construction of the anti-windup system corresponds to the addition of a saturation function to (9). The saturation function is set with the lower and upper limits of the actuators. The LQR controller with an anti-windup system has the following form:

$$\tilde{\mathbf{u}}(k) = \mathbf{u}(k-1) + \mathbf{K}\left(\mathbf{x}(k-1) - \mathbf{x}(k)\right) - \bar{\mathbf{K}}\mathbf{e}(k-1)$$
$$\mathbf{u}(k) = f(\tilde{\mathbf{u}}(k)) \quad (10)$$

with

$$f(\tilde{\mathbf{u}}(k)) = \begin{cases} \tilde{\mathbf{u}}(k), & \mathbf{u}_{\min} \le \tilde{\mathbf{u}}(\text{k}) \le \mathbf{u}_{\max} \\ \mathbf{u}_{\max}, & \tilde{\mathbf{u}}(\text{k}) > \mathbf{u}_{\max} \\ \mathbf{u}_{\min}, & \tilde{\mathbf{u}}(k) < \mathbf{u}_{\min} \end{cases}$$

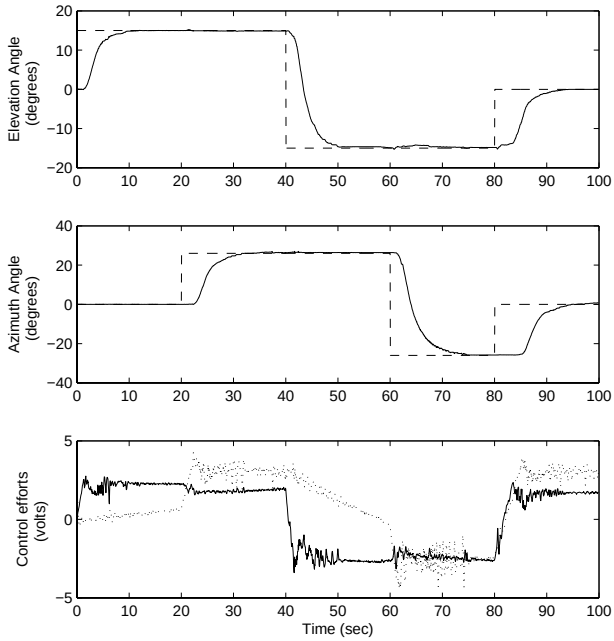

Fig. 6. LQG control system applied to the helicopter laboratory process in nominal conditions. The amplitudes of the setpoint sequences are 15 degrees for the elevation angle and 26 degrees for the azimuth angle. In the first two plots: (− −) reference trajectory (—) Helicopter's trajectory. In the third plot the control voltages: main rotor (—) and side rotor ($\cdots$).

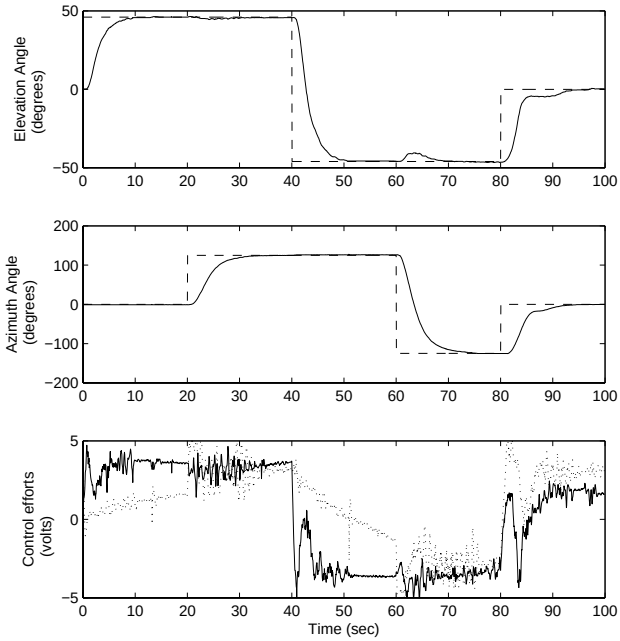

Fig. 7. LQG control system applied to the helicopter laboratory process in nominal conditions. The amplitudes of the setpoint sequences are 46 degrees for the elevation angle and 124.8 degrees for the azimuth angle. In the first two plots: (− −) reference trajectory (—) Helicopter's trajectory. In the third plot the control voltages: main rotor (—) and side rotor ($\cdots$).

where $\mathbf{u}_{\min}$ is the vector of the actuators lower limits, $\mathbf{u}_{\max}$ is the vector of the actuators upper limits, and $\mathbf{e}(k) = \mathbf{r}(k) - \mathbf{y}(k)$ is the tracking error.

The block scheme of the LQR with integral action and anti-windup system is shown in Fig. 4. Since $\mathbf{u}(k)$ will become $\mathbf{u}(k-1)$ in the next sampling time, the saturator avoids that $\mathbf{u}(k)$ grows up beyond the actuator limits by stopping the integration when it is needed.

3.3 Experimental Results

The control system was implemented entirely in *Simulink* using the *Real-Time windows target 2.2* [13] and the *Real-Time windows workshop 5.0* [14] of *Matlab*. The interface between the PC with *Simulink* and the helicopter was made using a data acquisition board (PCI-1200) manufactured by *National Instruments*. The sampling time for the control system was 50 ms.

In order to evaluate the performance of the control system, the setpoint sequences shown in Fig. 5 were used. Fig. 6 shows the response of the controlled system when the setpoints are 15 degrees for the elevation angle and 26 degrees for the azimuth angle. In the same way, Fig. 7 presents the results obtained when the setpoints for the elevation and azimuth angles are 46 degrees and 124.8 degrees respectively. The results presented in those figures have been obtained working with the helicopter in nominal conditions (without serious disturbances), i.e. under the same conditions as when it was identified. In general terms the LQG controller presents a good nominal behavior. The system response does not exhibit overshoot, the control actions are within their operating ranges and the degree of influence between the azimuth angle changes and the elevation angle is small (check the plots between 60 and 80 sec).

In order to test the ability of the control system of dealing with process disturbances, the position of one of the helicopter counterweights was modified as is depicted in Fig 8. As consequence of this, the equilibrium position of the lever arm with respect to the vertical axle (elevation angle) changed from 0 degrees to -29.9 degrees. Fig. 9 shows the response of the controlled system in disturbed conditions when the setpoints for the elevation and azimuth angles are 15 and 26 degrees respectively. It is clear that the system shows some oscillations in steady state (see the plots in Fig. 9 between 0 and 40 sec) when the LQG controller is operating with small setpoints for the elevation angle. The performance of the linear controller (settling times, overshoots, and so on) is clearly affected by the changes. Fig. 9 shows that the azimuth angle is practically unaffected by the change in the counterweight position, whereas the elevation angle is affected in a negative way.

We carried out several experiments by moving the counterweight to intermediate positions, but the most critical situation where the performance of the LQG controller was degraded the most is the one shown in

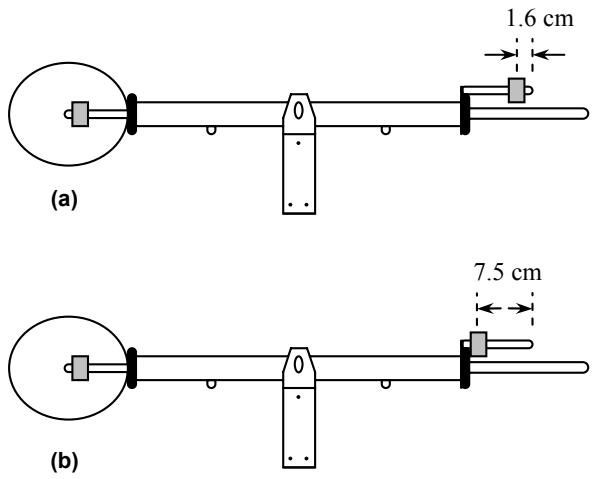

Fig. 8. Position of the counterweights. (a) Nominal conditions. (b) Disturbed conditions.

Fig. 8. It is clear that the changes accentuated the nonlinearities of the process.

In order to overcome this situation, we have to design a controller that takes into account the nonlinear behavior of the helicopter along all the operating range of the elevation angle. A way of doing this is through a TS fuzzy controller which is designed from the TS fuzzy model of process. This TS fuzzy model would be built by integrating a set of linear models that would be derived by identifying the process around different elevation angles (the operating point of the azimuth angle would be kept constant). This is the approach that we followed, and it will be presented in detail in the next section.

4 Fuzzy Control System

In this study a TS fuzzy controller was designed by using the concept of Parallel Distributed Compensation (PDC) [22]. Since the use of PDC requires having the TS fuzzy model of the process, the first step in the design of the control system was the derivation of the TS fuzzy model of the helicopter. A TS fuzzy model can be obtained in many ways; if a nonlinear rigorous model is available the model can be extracted by linearizing the process around different operating points. If this is not the case, we can construct the fuzzy model by using linear system identification techniques, which allow us to estimate the local linear models. In our case the second option was chosen [1][2].

4.1 Takagi-Sugeno Fuzzy Model of the Helicopter

Given that the changes in the position of the counterweights affects mainly the elevation angle ($y_1(k)$), this angle was selected as the premise variable in the fuzzy rules. In order to minimize the design effort and complexity, we used as few rules as possible. The number of rules and consequently the number of local linear models was set to three. Schemes using five rules were tested without significant improvements.

In a similar fashion as it was explained in section 3.1, the helicopter was identified around three operating points: -30 degrees, 0 degrees and 30 degrees of elevation angle and 0 degrees of azimuth angle. Once the local models were derived they were integrated into a global TS fuzzy model. This fuzzy model is defined as follows:

$$\begin{aligned}
&\text{IF } y_1 \text{ is } \mathrm{M}_1 \text{ THEN } \mathbf{x}(k+1) = \mathbf{A}_1\mathbf{x}(k) + \mathbf{B}_1\mathbf{u}(k)\\
&\text{IF } y_1 \text{ is } \mathrm{M}_2 \text{ THEN } \mathbf{x}(k+1) = \mathbf{A}_2\mathbf{x}(k) + \mathbf{B}_2\mathbf{u}(k)\\
&\text{IF } y_1 \text{ is } \mathrm{M}_3 \text{ THEN } \mathbf{x}(k+1) = \mathbf{A}_3\mathbf{x}(k) + \mathbf{B}_3\mathbf{u}(k)
\end{aligned} \quad (11)$$

$$\mathbf{y}(k) = \begin{bmatrix} 1 & 0 & 0 & 0 & 0 & 0 & 0 \\ 0 & 0 & 0 & 0 & 0 & 0 & 1 \end{bmatrix} \mathbf{x}(k)$$

with

$$\mathbf{A}_1 = \begin{bmatrix} 0 & 1 & 0 & 0 & 0 & 0 & 0 \\ 0 & 0 & 1 & 0 & 0 & 0 & 0 \\ 0.867 & -2.726 & 2.86 & 0 & 0 & 0 & 0 \\ 0 & 0 & 0 & 0 & 1 & 0 & 0 \\ 0 & 0 & 0 & 0 & 0 & 1 & 0 \\ 0 & 0 & 0 & 0.647 & -2.236 & 2.587 & 0 \\ 0 & 0 & 0 & 0 & 0.05 & 0 & 1 \end{bmatrix}$$

$$\mathbf{A}_2 = \begin{bmatrix} 0 & 1 & 0 & 0 & 0 & 0 & 0 \\ 0 & 0 & 1 & 0 & 0 & 0 & 0 \\ 0.808 & -2.61 & 2.802 & 0 & 0 & 0 & 0 \\ 0 & 0 & 0 & 0 & 1 & 0 & 0 \\ 0 & 0 & 0 & 0 & 0 & 1 & 0 \\ 0 & 0 & 0 & 0.759 & -2.474 & 2.714 & 0 \\ 0 & 0 & 0 & 0 & 0.05 & 0 & 1 \end{bmatrix}$$

$$\mathbf{A}_3 = \begin{bmatrix} 0 & 1 & 0 & 0 & 0 & 0 & 0 \\ 0 & 0 & 1 & 0 & 0 & 0 & 0 \\ 0.884 & -2.76 & 2.878 & 0 & 0 & 0 & 0 \\ 0 & 0 & 0 & 0 & 1 & 0 & 0 \\ 0 & 0 & 0 & 0 & 0 & 1 & 0 \\ 0 & 0 & 0 & 0.6236 & -2.176 & 2.55 & 0 \\ 0 & 0 & 0 & 0 & 0.05 & 0 & 1 \end{bmatrix}$$

$$\mathbf{B}_1 = \begin{bmatrix} -1.527 \cdot 10^{-3} & -1.008 \cdot 10^{-4} \\ -3.925 \cdot 10^{-4} & -3.5 \cdot 10^{-4} \\ 7.525 \cdot 10^{-4} & -5.653 \cdot 10^{-4} \\ 0 & 3.047 \cdot 10^{-3} \\ 0 & 2.888 \cdot 10^{-3} \\ 0 & 3.18 \cdot 10^{-3} \\ 0 & 1.523 \cdot 10^{-4} \end{bmatrix}$$

$$\mathbf{B}_2 = \begin{bmatrix} 2.007 \cdot 10^{-4} & -2.511 \cdot 10^{-4} \\ 3.86 \cdot 10^{-4} & -6.396 \cdot 10^{-4} \\ 6.548 \cdot 10^{-4} & -9.555 \cdot 10^{-4} \\ 0 & 1.947 \cdot 10^{-3} \\ 0 & 1.419 \cdot 10^{-3} \\ 0 & 1.388 \cdot 10^{-3} \\ 0 & 9.735 \cdot 10^{-5} \end{bmatrix}$$

$$\mathbf{B}_3 = \begin{bmatrix} -1.711 \cdot 10^{-3} & -4.506 \cdot 10^{-4} \\ -6.866 \cdot 10^{-4} & -7.975 \cdot 10^{-4} \\ 3.707 \cdot 10^{-4} & -1.095 \cdot 10^{-3} \\ 0 & 3.153 \cdot 10^{-3} \\ 0 & 2.155 \cdot 10^{-3} \\ 0 & 2.13 \cdot 10^{-3} \\ 0 & 1.577 \cdot 10^{-4} \end{bmatrix}$$

where $\mathbf{x}(k) \in \Re^7$ is the state vector, ($\mathbf{A}_1 \in \Re^{7\times7}$, $\mathbf{B}_1 \in \Re^{7\times2}$), ($\mathbf{A}_2 \in \Re^{7\times7}$, $\mathbf{B}_2 \in \Re^{7\times2}$) and ($\mathbf{A}_3 \in \Re^{7\times7}$, $\mathbf{B}_3 \in \Re^{7\times2}$) are the matrices describing the local dynamics, $\mathbf{y}(k) \in \Re^2$ is the output vector ($y_1(k)$ is the elevation angle and $y_2(k)$ is the azimuth angle), $\mathbf{u}(k) \in \Re^2$ is the input vector ($u_1(k)$ and $u_2(k)$ are the voltages applied

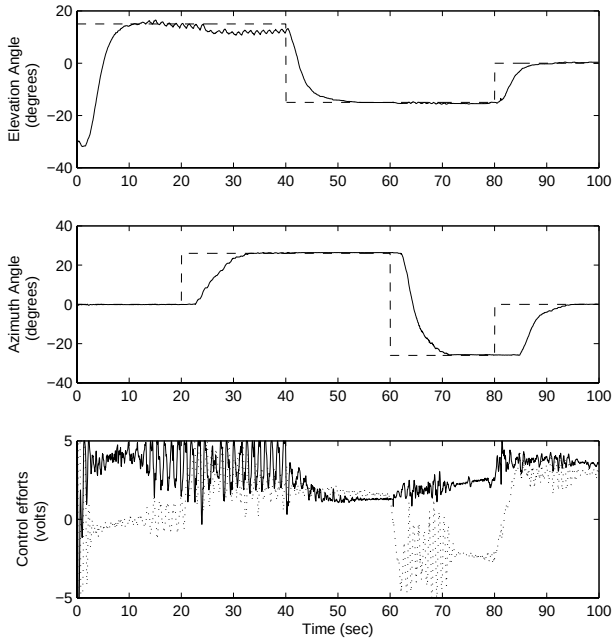

Fig. 9. LQG control system applied to the helicopter laboratory process in disturbed conditions. The amplitudes of the setpoint sequences are 15 degrees for the elevation angle and 26 degrees for the azimuth angle. In the first two plots: (− −) reference trajectory (—) Helicopter's trajectory. In the third plot the control voltages: main rotor (—) and side rotor ($\cdots$).

to the main and side rotors respectively) and M_1, M_2 and M_3 are the membership functions of the elevation angle which are shown in Fig. 10.

It is very important to remark that all the local state space representations on which the TS fuzzy model is based, must have in common the state vector $\mathbf{x}(k)$, i.e. they have to be consistent. For this reason the identification algorithm was configured to produce state space models in an observer canonical form (check section 3.1). As consequence of this, the matrices $\mathbf{A}_i$ have certain common structure and the matrix $\mathbf{C}$ is common for all the local models.

The stability of the fuzzy model can be analyzed using the conditions given in the following theorem [17]:

Theorem 1 *The equilibrium of a discrete TS fuzzy system is asymptotically stable in the large if there exists a common positive definite matrix* $\mathbf{P}$ *such that*

$$\mathbf{A}_i^T \mathbf{P} \mathbf{A}_i - \mathbf{P} < \mathbf{0}, \quad \text{for } i = 1, 2, \ldots, N$$

where N *is the number of rules and* $\mathbf{A}_i$ *is the matrix governing the dynamics of the* i*th subsystem.*

This stability problem can be reduced to an LMI problem that can be solved numerically in a very efficient way [7][11][16][22]. Since all the local linear models are marginally stable (there is an integrator in each linear model) in our case, it is expectable that the equilibrium of the TS fuzzy model of the helicopter not be asymptotically stable in the large.

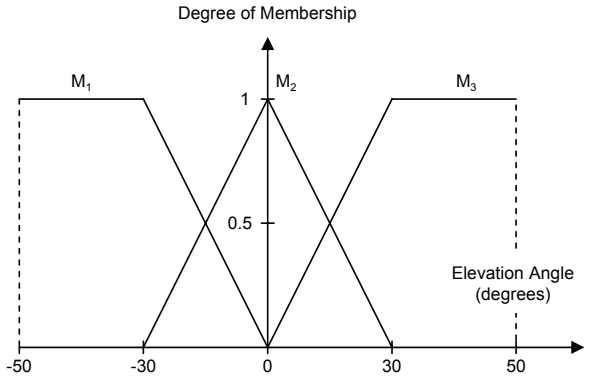

Fig. 10. Membership functions of the fuzzy model.

4.2 Takagi-Sugeno Fuzzy Controller

The concept of parallel distributed compensation proposes to design a linear compensator and a linear observer for each rule of the TS fuzzy model [17][11]. One important point is that the fuzzy observer and the fuzzy controller can be designed separately [11]. The design involves an iterative process. Once the local controllers are calculated, an LMI-based stability analysis (see Theorem 2) is carried out to check whether the closed-loop system (TS fuzzy controller + TS fuzzy model) is stable. If the system is unstable, the linear controller for each rule is redesigned usually by relaxing the goals for the local controllers. In the same way once the local observers are calculated, an LMI-based stability analysis (see Theorem 3) must be performed in order to check the stability of the TS fuzzy observer. If the fuzzy observer is unstable, the linear observer for each rule is redesigned by assuming a larger covariance of the states. The design procedure is simple and intuitive. The stability theorems for the closed loop system are reproduced in the following lines:

Theorem 2 *The equilibrium of a system composed by a TS fuzzy controller and a TS Fuzzy Model is asymptotically stable in the large, if there exists a common positive definite matrix* $\mathbf{P}$ *that satisfies the following matrix inequalities [22]:*

$$(\mathbf{A}_i - \mathbf{B}_i\mathbf{K}_i)^T \mathbf{P} (\mathbf{A}_i - \mathbf{B}_i\mathbf{K}_i) - \mathbf{P} < \mathbf{0}, \quad i = 1, \ldots, N$$

$$\mathbf{G}_{ij}^T \mathbf{P} \mathbf{G}_{ij} - \mathbf{P} < \mathbf{0}, \quad i < j \leq N$$

with

$$\mathbf{G}_{ij} = \frac{(\mathbf{A}_i - \mathbf{B}_i\mathbf{K}_j) + (\mathbf{A}_j - \mathbf{B}_j\mathbf{K}_i)}{2}, \quad i < j$$

where N *is the number of rules,* $\mathbf{A}_i$ *and* $\mathbf{B}_i$ *are the matrices describing each local model and* $\mathbf{K}_i$ *is the local controller gain.*

Theorem 3 *A fuzzy observer is asymptotically stable if there exists a common positive definite matrix* $\mathbf{Q}$ *that satisfies the following condition [16][11]:*

$$(\mathbf{A}_i - \mathbf{L}_i\mathbf{C})^T \mathbf{Q} (\mathbf{A}_i - \mathbf{L}_i\mathbf{C}) - \mathbf{Q} < \mathbf{0}, \quad i = 1, 2, \ldots, N$$

where N is the number of rules, $\mathbf{A}_i$ and $\mathbf{B}_i$ are the matrices describing each local model and $\mathbf{L}_i$ is the local observer gain.

As in the case of Theorem 1, these last theorems can also be recast as LMI problems in order to be solved numerically.

The block diagram of the implemented control system can be observed in Fig. 11. The local linear controllers on which the TS fuzzy controller with integral action is based were designed using optimal control techniques (LQR). In a similar way, the local observers on which the TS fuzzy observer is based were calculated using optimal estimation methods (Kalman filter). The inclusion of integral terms ("TS fuzzy integrator" block) in the fuzzy controller is necessary for avoiding steady state errors in the elevation and azimuth angles.

For designing the TS fuzzy controller with integral action is firstly required to find the augmented description of each local model. This augmented description is given by the following equation:

$$\begin{bmatrix} \mathbf{x}(k+1) \\ \mathbf{x}_\mathrm{e}(k+1) \end{bmatrix} = \begin{bmatrix} \mathbf{A}_i & \mathbf{0} \\ -\mathbf{C} & \mathbf{I} \end{bmatrix} \begin{bmatrix} \mathbf{x}(k) \\ \mathbf{x}_\mathrm{e}(k) \end{bmatrix} + \tag{12}$$

$$+ \begin{bmatrix} \mathbf{B}_i \\ \mathbf{0} \end{bmatrix} \mathbf{u}(k) + \begin{bmatrix} \mathbf{0} \\ \mathbf{I} \end{bmatrix} \mathbf{r}(k), \quad i = 1, 2, 3$$

where $\mathbf{r}(k) \in \Re^2$ is the vector of references and $\mathbf{x}_\mathrm{e}(k) \in \Re^2$ represents the extra states introduced to the local models by two integral terms (integrator form: $1/(z-1)$). These integral terms reduce to zero the steady state errors of the elevation and azimuth angles.

Dealing with the augmented description of each local model we calculated the controllers' feedback gains and checked the stability of the closed-loop system by solving the LMI problem associated to Theorem 2. We found the following positive definite matrix $\mathbf{P} \in \Re^{9\times 9} = \begin{bmatrix} \mathbf{P}_1 & \mathbf{P}_2 \end{bmatrix}$,

$$\mathbf{P}_1 = \begin{bmatrix} 37.6793 & -81.4063 & 43.9719 & 0.7472 & -1.9397 \\ -81.4063 & 177.1822 & -96.3487 & -1.7447 & 4.4094 \\ 43.9719 & -96.3487 & 52.7185 & 0.9980 & -2.4666 \\ 0.7472 & -1.7447 & 0.9980 & 33.4593 & -76.3662 \\ -1.9397 & 4.4094 & -2.4666 & -76.3662 & 176.8351 \\ 1.3338 & -2.9868 & 1.6474 & 44.4398 & -104.1067 \\ 0.1746 & -0.4042 & 0.2290 & 1.2926 & -3.1554 \\ -0.0026 & 0.0067 & -0.0043 & 0.0010 & -0.0026 \\ -0.0025 & 0.0055 & -0.0031 & -0.0216 & 0.0515 \end{bmatrix}$$

$$\mathbf{P}_2 = \begin{bmatrix} 1.3338 & 0.1746 & -0.0026 & -0.0025 \\ -2.9868 & -0.4042 & 0.0067 & 0.0055 \\ 1.6474 & 0.2290 & -0.0043 & -0.0031 \\ 44.4398 & 1.2926 & 0.0010 & -0.0216 \\ -104.1067 & -3.1554 & -0.0026 & 0.0515 \\ 61.9588 & 2.0028 & 0.0017 & -0.0328 \\ 2.0028 & 0.2703 & 0.0003 & -0.0036 \\ 0.0017 & 0.0003 & 9.5\cdot 10^{-6} & -7.23\cdot 10^{-6} \\ -0.0328 & -0.0036 & -7.23\cdot 10^{-6} & 0.0002 \end{bmatrix}$$

that guarantees the stability of the closed-loop system. The TS fuzzy controller with integral action has the following form:

$$\begin{aligned} &\text{IF } y_1 \text{ is } \mathrm{M}_1 \text{ THEN } \mathbf{u}(k) = -\mathbf{K}_1\mathbf{x}(k) - \bar{\mathbf{K}}_1\mathbf{x}_\mathrm{e}(k) \\ &\text{IF } y_1 \text{ is } \mathrm{M}_2 \text{ THEN } \mathbf{u}(k) = -\mathbf{K}_2\mathbf{x}(k) - \bar{\mathbf{K}}_2\mathbf{x}_\mathrm{e}(k) \\ &\text{IF } y_1 \text{ is } \mathrm{M}_3 \text{ THEN } \mathbf{u}(k) = -\mathbf{K}_3\mathbf{x}(k) - \bar{\mathbf{K}}_3\mathbf{x}_\mathrm{e}(k) \end{aligned} \tag{13}$$

with

$$\mathbf{K}_1^T = \begin{bmatrix} 207.4202 & 2.6377 \\ -450.6139 & -5.3594 \\ 245.7918 & 2.6584 \\ 2.4037 & 67.2075 \\ -5.9272 & -166.9110 \\ 3.7713 & 107.4875 \\ 0.1949 & 8.0096 \end{bmatrix}, \quad \bar{\mathbf{K}}_1 = \begin{bmatrix} -0.0489 & -0.0019 \\ 0.0021 & -0.1116 \end{bmatrix}$$

$$\mathbf{K}_2^T = \begin{bmatrix} 319.5495 & 4.7252 \\ -721.2870 & -9.4351 \\ 406.4029 & 4.3596 \\ 13.0903 & 107.4951 \\ -29.7839 & -246.0480 \\ 17.5491 & 146.1810 \\ 0.6300 & 7.0729 \end{bmatrix}, \quad \bar{\mathbf{K}}_2 = \begin{bmatrix} -0.0768 & -0.0063 \\ 0.0066 & -0.0966 \end{bmatrix}$$

$$\mathbf{K}_3^T = \begin{bmatrix} 401.0368 & 3.2555 \\ -875.1871 & -4.3287 \\ 480.1316 & 0.3872 \\ 6.1652 & 48.1934 \\ -15.4439 & -121.1675 \\ 10.0943 & 79.7192 \\ 0.7294 & 6.9327 \end{bmatrix}, \quad \bar{\mathbf{K}}_3 = \begin{bmatrix} -0.0949 & -0.0084 \\ 0.0134 & -0.0963 \end{bmatrix}$$

where $y_1(k) \in \Re$ is the elevation angle, M_1, M_2 and M_3 are the membership functions which are shown in Fig. 10, $\mathbf{x}_\mathrm{e}(k) \in \Re^2$ is the state vector of the integrators, $\mathbf{x}(k) \in \Re^7$ is the state vector of the process that in practice is estimated by a TS fuzzy observer ($\hat{\mathbf{x}}(x)$), $\mathbf{K}_1 \in \Re^{2\times 7}$, $\mathbf{K}_2 \in \Re^{2\times 7}$ and $\mathbf{K}_3 \in \Re^{2\times 7}$ are the state-feedback gain matrices and $\bar{\mathbf{K}}_1 \in \Re^{2\times 2}$, $\bar{\mathbf{K}}_2 \in \Re^{2\times 2}$ and $\bar{\mathbf{K}}_3 \in \Re^{2\times 2}$ are the integral gain matrices of the local controllers.

The output of the TS fuzzy controller is given by

$$\mathbf{u}(k) = -\sum_{i=1}^{N} h_i(k) \left(\mathbf{K}_i\mathbf{x}(k) + \bar{\mathbf{K}}_i\mathbf{x}_\mathrm{e}(k) \right) \tag{14}$$

$$h_i(k) = \mu_i(y_1(k)) \Big/ \sum_{i=1}^{N} \mu_i(y_1(k))$$

where $\mu_i(y_i(k))$ is the membership degree of $y_i(k)$ in the set M_i and N is the number of rules.

As it was mentioned before, we calculated the observers gains using optimal estimation techniques and we checked the stability of the TS fuzzy observer via LMI (see Theorem 3). We found the following positive definite matrix $\mathbf{Q} \in \Re^{7\times 7} = \begin{bmatrix} \mathbf{Q}_1 & \mathbf{Q}_2 \end{bmatrix}$,

$$\mathbf{Q}_1 = \begin{bmatrix} 92.9371 & -164.3379 & 76.5106 & -3.5669 \\ -164.3379 & 330.6202 & -163.0996 & 8.3192 \\ 76.5106 & -163.0996 & 82.8381 & -3.5411 \\ -3.5669 & 8.3192 & -3.5411 & 32.4358 \\ 9.5476 & -18.8698 & 8.1802 & -61.9131 \\ -5.8730 & 11.0107 & -4.9467 & 29.8816 \\ -0.0813 & -2.7092 & 1.7401 & -1.3333 \end{bmatrix}$$

$$\mathbf{Q}_2 = \begin{bmatrix} 9.5476 & -5.8730 & -0.0813 \\ -18.8698 & 11.0107 & -2.7092 \\ 8.1802 & -4.9467 & 1.7401 \\ -61.9131 & 29.8816 & -1.3333 \\ 134.7148 & -69.5500 & -17.6858 \\ -69.5500 & 37.4138 & 9.7702 \\ -17.6858 & 9.7702 & 87.3383 \end{bmatrix}$$

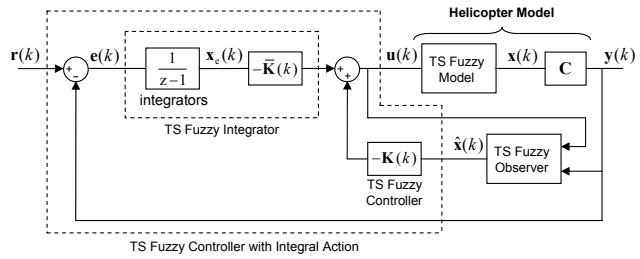

Fig. 11. Block diagram of the fuzzy control system (servo control).

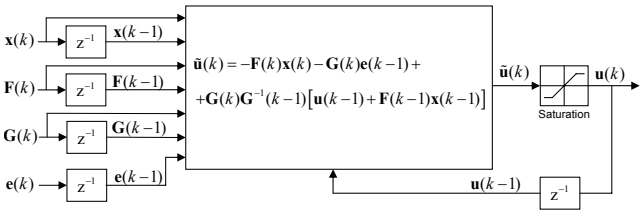

Fig. 12. Block scheme of the TS fuzzy controller with Integral action and anti-windup system.

which certifies the stability of fuzzy observer. The TS fuzzy observer has the following structure:

$$\begin{aligned}
&\text{IF } y_1 \text{ is } \mathrm{M}_1 \text{ THEN } \hat{\mathbf{x}}(k+1) = \mathbf{A}_1\hat{\mathbf{x}}(k) + \\
&\qquad + \mathbf{B}_1\mathbf{u}(k) + \mathbf{L}_1(\mathbf{y}(k) - \hat{\mathbf{y}}(k)) \\
&\text{IF } y_1 \text{ is } \mathrm{M}_2 \text{ THEN } \hat{\mathbf{x}}(k+1) = \mathbf{A}_2\hat{\mathbf{x}}(k) + \\
&\qquad + \mathbf{B}_2\mathbf{u}(k) + \mathbf{L}_2(\mathbf{y}(k) - \hat{\mathbf{y}}(k)) \\
&\text{IF } y_1 \text{ is } \mathrm{M}_3 \text{ THEN } \hat{\mathbf{x}}(k+1) = \mathbf{A}_3\hat{\mathbf{x}}(k) + \\
&\qquad + \mathbf{B}_3\mathbf{u}(k) + \mathbf{L}_3(\mathbf{y}(k) - \hat{\mathbf{y}}(k))
\end{aligned} \tag{15}$$

$$\hat{\mathbf{y}}(k) = \begin{bmatrix} 1 & 0 & 0 & 0 & 0 & 0 & 0 \\ 0 & 0 & 0 & 0 & 0 & 0 & 1 \end{bmatrix} \hat{\mathbf{x}}(k)$$

with

$$\mathbf{L}_1 = \begin{bmatrix} 1.0719 & -0.0194 \\ 1.3545 & -0.0188 \\ 1.6292 & -0.0071 \\ -0.0657 & 3.2104 \\ -0.0819 & 3.5934 \\ -0.1031 & 3.9702 \\ -0.0061 & 0.6370 \end{bmatrix}, \quad \mathbf{L}_2 = \begin{bmatrix} 0.7173 & 0.0321 \\ 0.9118 & 0.0674 \\ 1.1064 & 0.1155 \\ 0.0984 & 3.1107 \\ 0.0845 & 3.5240 \\ 0.0179 & 3.9332 \\ 0.0098 & 0.6232 \end{bmatrix}$$

$$\mathbf{L}_3 = \begin{bmatrix} 1.0772 & 0.0088 \\ 1.3581 & 0.0396 \\ 1.6340 & 0.0858 \\ -0.0307 & 3.4159 \\ -0.0378 & 3.8437 \\ -0.0715 & 4.2709 \\ -0.0031 & 0.6603 \end{bmatrix}$$

where $y_1(k) \in \Re$ is the elevation angle, M_1, M_2 and M_3 are the membership functions that are shown in Fig. 10, $\hat{\mathbf{x}}(k) \in \Re^7$ is the estimated state vector of the process, ($\mathbf{A}_1 \in \Re^{7\times7}$, $\mathbf{B}_1 \in \Re^{7\times2}$), ($\mathbf{A}_2 \in \Re^{7\times7}$, $\mathbf{B}_2 \in \Re^{7\times2}$) and ($\mathbf{A}_3 \in \Re^{7\times7}$, $\mathbf{B}_3 \in \Re^{7\times2}$) are the matrices describing the local dynamics given in (11), $\mathbf{L}_1 \in \Re^{7\times2}$, $\mathbf{L}_2 \in \Re^{7\times2}$ and $\mathbf{L}_3 \in \Re^{7\times2}$ are the observers gains, and $\mathbf{u}(k)$ and $\mathbf{y}(k)$ are respectively the input and output vectors of the process.

4.2.1 Anti-windup system

As in the LQR case presented in section 3.2.1, the first step in the implementation of the anti-windup mechanism for the fuzzy controller is to transform it into a recursive form [1]. This procedure is presented in the following lines. If we define the following matrices,

$$\mathbf{F}(k) = \sum_{i=1}^{N} h_i(k)\mathbf{K}_i \quad \text{and} \quad \mathbf{G}(k) = \sum_{i=1}^{N} h_i(k)\bar{\mathbf{K}}_i \tag{16}$$

then equation (14) can be written as follows,

$$\mathbf{u}(k) = -\mathbf{F}(k)\mathbf{x}(k) - \mathbf{G}(k)\mathbf{x}_\mathrm{e}(k). \tag{17}$$

Now, we can replace the differences equation of the integral terms ($\mathbf{x}_\mathrm{e}(k) = \mathbf{x}_\mathrm{e}(k-1) + \mathbf{e}(k-1)$ from $1/(z-1)$) in (17) as follows,

$$\mathbf{u}(k) = -\mathbf{F}(k)\mathbf{x}(k) - \mathbf{G}(k)\mathbf{e}(k-1) - \mathbf{G}(k)\mathbf{x}_\mathrm{e}(k-1). \tag{18}$$

From (17), and assuming that the matrix $\mathbf{G}(k)$ is square (usually it is if the number of references equals the degrees of freedom of the system) and non-singular for all k, we can write

$$\mathbf{x}_\mathrm{e}(k-1) = -\mathbf{G}^{-1}(k-1)\left[\mathbf{u}(k-1) + \mathbf{F}(k-1)\mathbf{x}(k-1)\right]. \tag{19}$$

Finally by replacing (19) in (18),

$$\begin{aligned}
\mathbf{u}(k) = &-\mathbf{F}(k)\mathbf{x}(k) - \mathbf{G}(k)\mathbf{e}(k-1) + \\
&+ \mathbf{G}(k)\mathbf{G}^{-1}(k-1)\left[\mathbf{u}(k-1) + \mathbf{F}(k-1)\mathbf{x}(k-1)\right]
\end{aligned} \tag{20}$$

we obtain the recursive version of the TS fuzzy controller with integral action. Equation (20) is valid only if the matrix $\mathbf{G}(k)$ is square and non-singular for all k. The last step in the creation of the anti-windup system is the addition of a saturation function to (20). This function is configured with the lower and upper limits of the actuators to avoid that the control efforts grow up indefinitely. The final form of the fuzzy controller with anti-windup system is as follows:

$$\begin{aligned}
\tilde{\mathbf{u}}(k) = &-\mathbf{F}(k)\mathbf{x}(k) - \mathbf{G}(k)\mathbf{e}(k-1) + \\
&+ \mathbf{G}(k)\mathbf{G}^{-1}(k-1)\left[\mathbf{u}(k-1) + \mathbf{F}(k-1)\mathbf{x}(k-1)\right] \\
\mathbf{u}(k) = &\, f(\tilde{\mathbf{u}}(k))
\end{aligned} \tag{21}$$

with

$$f(\tilde{\mathbf{u}}(k)) = \begin{cases} \tilde{\mathbf{u}}(k), & \mathbf{u}_{\min} \le \tilde{\mathbf{u}}(k) \le \mathbf{u}_{\max} \\ \mathbf{u}_{\max}, & \tilde{\mathbf{u}}(k) > \mathbf{u}_{\max} \\ \mathbf{u}_{\min}, & \tilde{\mathbf{u}}(k) < \mathbf{u}_{\min} \end{cases}$$

where $\mathbf{u}_{\min}$ is the vector of the actuators lower limits and $\mathbf{u}_{\max}$ is the vector of the actuators upper limits. The block diagram of the TS fuzzy controller with integral action and anti-windup system is shown in Fig. 12. Since $\mathbf{u}(k)$ will become $\mathbf{u}(k-1)$ in the next sampling time, the saturator avoids that $\mathbf{u}(k)$ grows up beyond the actuator limits by stopping the integration when it is needed.

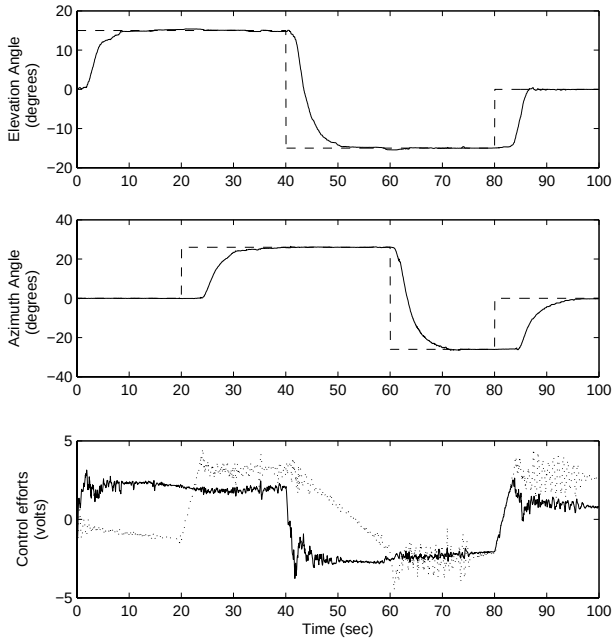

Fig. 13. TS fuzzy controller applied to the helicopter laboratory process in nominal conditions. The amplitudes of the setpoint sequences are 15 degrees for the elevation angle and 26 degrees for the azimuth angle. In the first two plots: (– –) reference trajectory (—) Helicopter's trajectory. In the third plot the control voltages: main rotor (—) and side rotor ($\cdots$).

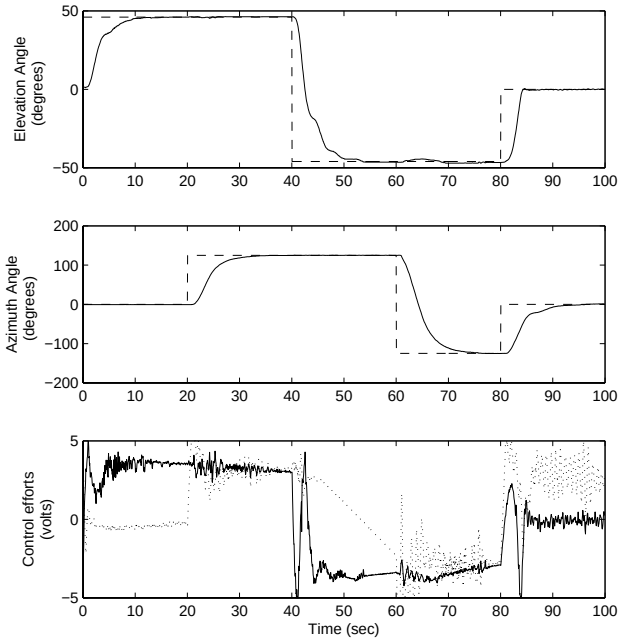

Fig. 14. TS fuzzy controller applied to the helicopter laboratory process in nominal conditions. The amplitudes of the setpoint sequences are 46 degrees for the elevation angle and 124.8 degrees for the azimuth angle. In the first two plots: (– –) reference trajectory (—) Helicopter's trajectory. In the third plot the control voltages: main rotor (—) and side rotor ($\cdots$).

During the real-time experiments, the matrix $\mathbf{G}(k)$ was always non-singular for the whole operating range of the helicopter. However no prior conditions for the non-singularity of $\mathbf{G}(k)$ has been derived yet, and it constitutes a topic of future research.

4.3 Experimental Results

For the implementation of the fuzzy control system the same hardware and software platform described in section 3.3 was used. In addition, the setpoint sequences shown in Fig. 5 were employed for evaluating the performance of the fuzzy controller. Fig. 13 shows the response of the controlled system when the setpoints are 15 degrees for the elevation angle and 26 degrees for the azimuth angle. Similarly, Fig. 14 presents the response of the controlled system when the setpoints for the elevation and azimuth angles are 46 and 124.8 degrees respectively. The results presented in those figures have been obtained working with the helicopter in nominal conditions (without serious disturbances), i.e. under the same conditions as when it was identified. In general terms the fuzzy control system presents a good behavior and it has similar settling times and control efforts than the LQG controller. However we can notice that the degree of influence between the azimuth angle changes and the elevation angle is smaller in the fuzzy control system than in the LQG controller (check the plots between 60 and 80 sec).

Fig. 15 shows the response of the fuzzy controller when the position of one of the counterweights was changed (see Fig. 8b - disturbed conditions). The new control system still has a good behavior in spite of the changes in the process dynamics as consequence of the change in the counterweight position. Notice that during the first 3 seconds of the experiment the helicopter exhibits an undershoot in the elevation angle. This situation is also observed when we are dealing with the LQG controller (see Fig. 9). Along all the experiments the initial state of the observers (linear and fuzzy) has been set to $\mathbf{0}$. Hence when the helicopter is operating in nominal conditions the initial value of the elevation angle is 0 degrees and the initial state of the process corresponds to the initial state of the observers. In this situation we do not observe any undershoot at the beginning of the experiments. When the helicopter is operating in disturbed conditions the initial value of the elevation angle is -29.9 degrees and we have a difference between the initial state of the process and the initial state of the observers. Since the observers require a couple of samples to converge to the correct state of the process, the controllers have to deal with bad estimations at the beginning of the tests. This leads to the generation of inappropriate control actions that cause the undershot observed in Fig. 9 and Fig. 15. We could get rid of the undershot by properly initializing the observers.

We have constructed a controller that can deal better with the changes in the counterweight position just by taking into account the nonlinear behavior of the

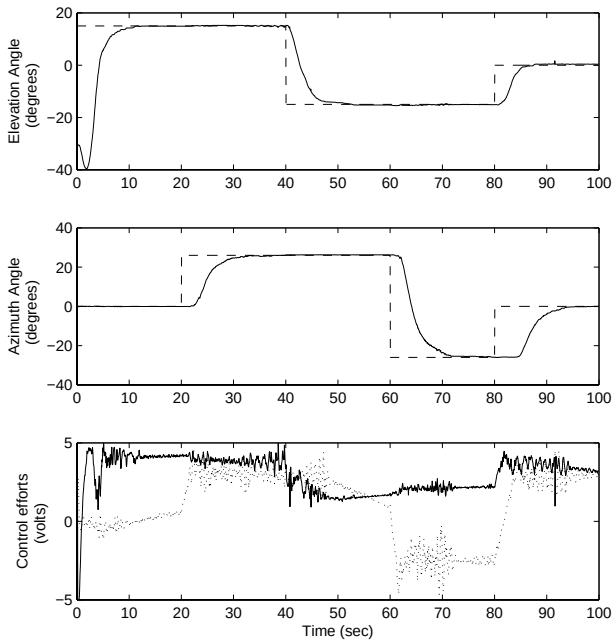

Fig. 15. TS fuzzy controller applied to the helicopter laboratory process in disturbed conditions. The amplitudes of the setpoint sequences are 15 degrees for the elevation angle and 26 degrees for the azimuth angle. In the first two plots: (– –) reference trajectory (—) Helicopter's trajectory. In the third plot the control voltages: main rotor (—) and side rotor ($\cdots$).

lever arm along its operating range through a TS fuzzy model, which is a nonlinear approximation of the real setup.

5 Conclusions

In this paper the experimental results of applying linear and fuzzy control techniques to a 2 degrees of freedom helicopter known as *COPTER II* have been presented. Additionally, a method to implement the anti-windup system for an LQG and a TS fuzzy controller has been derived.

Initially an LQG controller was designed from the linear model of the plant, which was found by means of subspace identification methods. Although the LQG was designed to work properly around an operating point, it showed to be suitable for working along the operating range of the helicopter when it is operating in nominal conditions. However when the helicopter dynamics was altered by changing the position of one counterweight, the LQG controller could not handle this change and the elevation angle of the helicopter exhibited oscillations around the reference point. In order to overcome this problem a more complex controller was designed by taking into account the dynamics of the plant along the operating range of the elevation angle. Therefore a TS fuzzy model was built from a set of local linear models, which were obtained using subspace identification techniques. Afterwards, the concept of parallel distributed compensation (PDC) was used to design a fuzzy controller and a fuzzy observer for the helicopter. The stability analyses in the design process were reduced to LMI problems.

The experimental results of the fuzzy control system were remarkable; the control system exhibited a good behavior both in nominal and disturbed conditions.

Finally we want to stress that in this paper a very practical approach has been used to control the process, where the modeling of the helicopter was done assuming no prior knowledge of the model structure and its parameters. This approach constitutes a good alternative for designing TS fuzzy controllers when the nonlinear model of the process is not available.

6 Acknowledgments

The authors would like to acknowledge the support of several institutions among others Vlaamse Interuniversiteit Raad and their project "Uitbouw van een uitmuntenheidcentrum en oprichting van een masters Degree in industriele controletechnieken in het noorden van Zuid Amerika". In addition, this research was supported by: • Research Council KUL: GOA AMBioRICS, CoE EF/05/006 Optimization in Engineering (OPTEC), IOF-SCORES4CHEM, several PhD/postdoc & fellow grants; • Flemish Government: ○ FWO: PhD/postdoc grants, projects G.0452.04 (new quantum algorithms), projects G.0499.04 (Statistics), G.0211.05 (Nonlinear), G.0226.06 (cooperative systems and optimization), G.0321.06 (Tensors), G.0302.07 (SVM/Kernel), G.0320.08 (convex MPC), G.0558.08 (Robust MHE), G.0557.08 (Glycemia2), research communities (ICCoS, ANMMM, MLDM); ○IWT: PhD Grants, McKnow-E, Eureka-Flite+; ○Helmholtz: viCERP; • Belgian Federal Science Policy Office: IUAP P6/04 (DYSCO, Dynamical systems, control and optimization, 2007-2011); • EU: ERNSI; FP7-HD-MPC (Collaborative Project STREP-grantnr. 223854) • Contract Research: AMINAL. Dr. Joos Vandewalle is a full professor at the Katholieke Universiteit Leuven, Belgium.

References

[1] O. M. Agudelo, *Control of a Helicopter Laboratory process using linear and fuzzy techniques*, M.S. dissertation, Universidad de Ibagué in cooperation with Universiteit Gent and Katholieke Universiteit Leuven, Ibagué, Colombia, 2003.

[2] O. M. Agudelo and J. J. Espinosa, *Identificación de un Helicóptero didáctico de dos grados de libertad*, in: Proceedings of the 5th congress of the Automation Colombian Association (ACA), Medellín, Colombia, 2003, CD-ROM.

[3] S. M. Ahmad, A. J. Chipperfield and M. O. Tokhi, *Modelling and Control of a Twin Rotor Multi-Input Multi-output System*, in: Proceedings of the American Control Conference (ACC2000), Chicago, IL, USA, 2000, 1720-1724.

[4] S. M. Ahmad, A. J. Chipperfield and M. O. Tokhi, *Dynamic modeling and Optimal Control of a Twin Rotor MIMO System*, in: Proceedings of the IEEE National Aerospace and Electronics Conference (NAECON2000), Dayton, Ohio, USA, 2000, 391-398.

[5] N. W. Aung, E. W. Cooper, Y. Hoshino and K. Kamei, A proposal of fuzzy control systems for trailers driven by multiple motors in side slipways to haul out ships, *International Journal of innovative Computing, Information and Control* **3**(4)(August 2007), 799-812.

[6] J. Balderud, *Modeling and control of a Toy-Helicopter*, M.S. dissertation, Karlstad University, Sweden, 2002.

[7] S. Boyd, L. El Ghaoui, E. Feron, and V. Balakrishnan, *Linear Matrix inequalities in systems and control theory*, vol. 15 of *Studies in Applied Mathematics*, SIAM, Philadelphia, PA, June 1994.

[8] C. Camayo and J. Arias, *Diseño y construcción de un módulo para control de posición angular con dos grados de libertad*, B.S. dissertation, Universidad Autónoma de Occidente, Cali, Colombia, 2002.

[9] H. Chu, K. Tsai and W. Chang, Fuzzy control of active queue management routers for transmission control protocol networks via time-delay affine Takagi-Sugeno fuzzy models, *International Journal of innovative Computing, Information and Control* **4**(2)(February 2008), 291-312.

[10] G. F. Franklin, J. D. Powell, and M. L. Workman, *Digital Control of Dynamic Systems*, Second Edition, Addison-Wesley, 1990.

[11] A. Jadbabaie, Robust, *Non-Fragile Controller synthesis using Model Based Fuzzy systems: A linear Matrix Inequalities Approach*, M.S. dissertation, University of New Mexico, USA, 1997.

[12] A. Rahideh, H. M. Shaheed, and A. H. Bajodah, Adaptive non-linear model inversion control of a twin rotor multi-input multi-output system using artificial intelligence, *Proceedings of the Institution of Mechanical Engineers, Part G: Journal of Aerospace Engineering* **221**(3) (2007), 343-351.

[13] *Real-Time Windows Target for use with Real-Time Workshop - User's guide version 2*, Mathworks, USA, 2002.

[14] *Real-Time Workshop for use with Simulink - User's guide version 5*, Mathworks, USA, 2002.

[15] P. Van Overschee and B. De Moor, *Subspace Identification of Linear Systems: Theory, Implementation, Applications*, Kluwer Academic Publishers, 1996.

[16] K. Tanaka, T. Ikeida, H. O. Wang, Fuzzy Regulators and Fuzzy Observers: Relaxed Stability Conditions and LMI-Based Designs, *IEEE Transactions on fuzzy systems* **6**(2) (May 1998), 250-256.

[17] K. Tanaka and M. Sugeno, Stability analysis and design of fuzzy control systems, *fuzzy Sets Syst.* **45**(2) (1992), 135-156.

[18] K. Tanaka, H. Ohtake and H.O. Wang, A practical Design approach to stabilization for 3DOF RC Helicopter, *IEEE Transactions on Control Systems Technology* **12**(2) (March 2004), 315-325.

[19] C. W. Tao, J. S. Taur, C. M. Wang and U. S. Chen, Fuzzy hierarchical swing-up and sliding position controller for the inverted pendulum-cart system, *Fuzzy Sets and Systems* **159**(20)(October 2008), 2763-2784.

[20] C. Tseng and C. Hwang, Fuzzy observer-based fuzzy control design for nonlinear systems with persistent bounded disturbances, *Fuzzy Sets and Systems* **158**(2)(January 2007), 164-179.

[21] S. Tong, P. Shi and H. Al-Madfai, Robust fuzzy decentralized control for nonlinear large-scale systems with parametric uncertainties, *Journal of Intelligent and Fuzzy Systems: Applications in Engineering and Technology* **19**(2)(April 2008), 85-101.

[22] H. O. Wang, K. Tanaka, and M. F. Griffing, An approach to fuzzy control of Nonlinear Systems: Stability and Design Issues, *IEEE Transactions on fuzzy systems* **4**(1) (February 1996), 14-23.

[23] M. Wang, B. Chen and S. Tong, Adaptive fuzzy tracking control for strict-feedback nonlinear systems with unknown time delays, *International Journal of innovative Computing, Information and Control* **4**(4)(April 2008), 829-838.